Theor Chem Account (2008) 120:429–435
DOI 10.1007/s00214-008-0418-7

REGULAR ARTICLE

Proton catalyzed hydrolytic deamination of cytosine: a computational study

V. Labet · A. Grand · C. Morell · J. Cadet · L. A. Eriksson

Received: 26 September 2007 / Accepted: 4 February 2008 / Published online: 26 February 2008

Abstract Two pathways involving proton catalyzed hydrolytic deamination of cytosine (to uracil) are investigated at the PCM-corrected B3LYP/6-311G(d,p) level of theory, in the presence of an additional catalyzing water molecule. It is concluded that the pathway involving initial protonation at nitrogen in position 3 of the ring, followed by water addition at C4 and proton transfer to the amino group, is a likely route to hydrolytic deamination. The rate determining step is the addition of water to the cytosine, with a calculated free energy barrier in aqueous solution of $\Delta G^{\neq}$=140 kJ/mol. The current mechanism provides a lower barrier to deamination than previous work based on OH^- catalyzed reactions, and lies closer to the experimental barrier derived from rate constants ($E_a = 117 \pm 4$ kJ/mol).

Keywords Cytosine · Hydrolytic deamination · B3LYP · Mutation · DNA

Dedicated to Professor Nino Russo on the occasion of his 60th birthday.

Electronic supplementary material The online version of this article (doi:10.1007/s00214-008-0418-7) contains supplementary material, which is available to authorized users.

V. Labet · A. Grand · C. Morell · J. Cadet
Laboratoire "Lésions des Acides Nucléiques",
DRFMC/SCIB, UMR-E 3 (CEA/UJF),
CEA-Grenoble, 17 avenue des Martyrs,
38054 Grenoble Cedex 9, France

L. A. Eriksson (✉)
Department of Natural Sciences and Örebro Life Science Center,
Örebro University, 701 82 Örebro, Sweden
e-mail: leif.eriksson@nat.oru.se

1 Introduction

The ordering of the main nucleobases in DNA, the pyrimidines cytosine and thymine (uracil in RNA) and the purines adenine and guanine, defines the genetic code of all living organisms. However, modified nucleobases in DNA and RNA are also well known to occur, either naturally in which case they often serve to provide a specific function or 'signal', or formed through unwanted reactions with various mutagenic agents [1]. In the case of the pyrimidine bases, cytosine is the one most susceptible to modification. Deamination of the N8 amine group (cf. Fig. 1) leads after hydrolysis to the formation of uracil, whereas the same reaction in the modified base 5-methylcytosine (5mC) leads to thymine. In each case, the deaminated base alters its hydrogen bonding pattern, such that it pairs better with adenine rather than guanine in the DNA stack, and hence upon transcription and replication gives rise to altered genetic material and coding for different amino acids relative to the parent sequence [2].

In addition to chemical modifications of the normal ("canonical") forms of the bases, various tautomeric forms of the nucleobases also exist. The different tautomers normally lie very close in energy. There are numerous theoretical [3–15] and experimental [16,17] studies exploring the relative stabilities and hydrogen bonding patterns of the tautomeric forms of cytosine, as well as mechanisms for the conversion between them. The relative stabilities of the different tautomers differ in gas phase compared to when including explicit water molecules as hydrogen bonding agents; most studies have hitherto focused on the 'normal' vs the 'enolic' form (with one of the N8 protons transferred to O7). Several studies of the interactions of the different tautomers with metal cations also exist [15,18–29].

Spontaneous hydrolytic deamination (induced by initial attack of either H^+, OH^-, or by H_2O itself) is a rare event

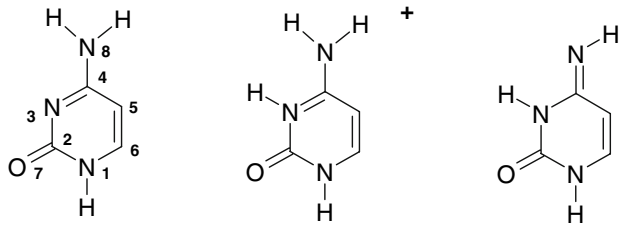

Fig. 1 Schematic models and atomic numbering of cytosine, N3 protonated form and imine tautomer of importance for the deamination pathways studied

under normal physiological conditions, and depends on both pH and temperature [30–33]. The presence of various reacting agents such as NO, bisulfite, and similar, increases the rate of deamination considerably [34,35]. Both acid- and base-catalyzed pathways to deamination have been proposed some 40 years ago [31,36] albeit the exact mechanism is still far from clear. Using genetic assay, Frederico et al. [37] determined the rate constants for deamination in single and double stranded DNA under physiological conditions. The value for the activation energy obtained, $E_a = 117 \pm 4$ kJ/mol, agrees well with an earlier value of $E_a = 121$ kJ/mol obtained over a temperature range of 25 deg [38]. Methylation of cytosine at C5 has been shown to increase the rate of deamination by a factor of 3–4 compared with normal cytosine [39], which has led to the notion of 5mC being 'hot spots' for mutations.

In a recent computational study, Almatarneh et al. [40] explored the hydrolytic deamination of cytosine in the gas-phase catalyzed by either a hydroxyl anion or a water molecule, by means of HF, MP2, B3LYP and G3MP2 levels of theory. A total of four different pathways were explored, and it was concluded that, even at the high level of theory G3MP2, all pathways gave too high activation parameters (lowest barriers of activation around $\Delta E_{act} = 148$ kJ/mol; $\Delta H^{\neq} = 146$ kJ/mol; $\Delta G^{\neq} = 156$ kJ/mol), compared with the experimental value of $E_a = 117 \pm 4$ kJ/mol [38]. The lowest barriers were obtained assuming an initial attack and binding by OH^- to C4, this also constituting the rate determining step. Interestingly, calculations at the B3LYP/6-31G(d,p) level gave 25–30 kJ/mol higher transition barriers than G3MP2. Although being some 30–40 kJ/mol too high, the barriers obtained by Almatarneh et al. are nonetheless considerably lower than those reported by Sponer et al. [22] in their study of OH^- induced deamination including bulk solvation effects. Metal- or metal enzyme mediated deamination has also been explored theoretically [22] and experimentally [41]. In their theoretical study, Sponer et al. showed that the presence of Pt^{II} plays a catalyzing role for the deamination reaction, decreasing the activation free energy of the rate-determining step from $\Delta G^{\neq} = 186$ kJ/mol in the case of nonmetalated cytosine to $\Delta G^{\neq} = 99$ kJ/mol in the case of a platinated cytosine [22].

In order to shed further light on possible mechanistic pathways of this important reaction, the deamination of cytosine based on acid (H^+) catalysis is in the current study explored theoretically, including both explicit water molecules and a polarized continuum model (PCM) for bulk solvation effects. Two different pathways are investigated, either assuming cytosine to be protonated at the N3 position, or assuming protonation to occur subsequent to water addition to neutral cytosine. The resulting barriers are considerably lower than those earlier reported for hydrolytic deamination, providing strong support for the current mechanisms as being chemically viable.

2 Methodology

All systems were geometry optimized using the hybrid Hartree–Fock–density functional theory functional B3LYP [42,43] in conjunction with the 6-311G(d,p) basis set [44–46]. Since all the systems studied in the current work are either neutral or positively charged, diffuse functions were judged as being of less importance compared to the increased computational time, and thus not included. As a first step, optimizations were carried out in gas phase, followed by optimizations including a polarized continuum model in the integral equation formalism (IEF-PCM; hereafter named PCM) [47–49], with dielectric constant $\varepsilon = 78.39$ to simulate the bulk effect of a polar environment. For PCM optimizations, the cavity was built using the United Atom Topologic Model applied on the atomic radii of the UFF force field, with 974 tesserae per sphere. In the cases where molecular systems had unbound hydrogens, the default cavity was modified by adding extra individual spheres on these atoms to the cavity built by default, using the keyword SPHEREONH.

Each stationary point was then characterized at the same level of theory of the one used for its optimization (B3LYP/6-311G(d,p) for stationary points optimized in gas phase and IEF-PCM/B3LYP/6-311G(d,p) for stationary points optimized using the PCM model) by computing the vibrational frequencies within the harmonic approximation. Thermodynamic data were extracted in order to obtain the Gibbs free energies of reaction and the corresponding activation energies at 298 K.

Intrinsic reaction coordinate (IRC) calculations were performed from each gas phase optimized transition structure at the same level of theory, to ensure that these connected to the appropriate reactants and products.

All calculations were performed using the Gaussian03 program [50].

3 Results and discussion

In the current study, two alternative routes to hydrolytic cytosine → uracil deamination are investigated. The first pathway assumes the cytosine moiety to be protonated at the N3 position (pathway A), and the second assumes the protonation to occur after water addition (pathway B). Cytosine, its N3 protonated form and the imine tautomer, as well as the atomic numbering used, are displayed in Fig. 1.

The nucleobases can exist in several different tautomeric forms that in general lie rather close in energy. For cytosine, the amino–oxo form (with N8 doubly protonated, and O7 and N3 un-protonated) is the most abundant one, but amino-hydroxo (protons on N8 and O7) and imine (protons on N8 and N3) forms also exist. Conversion between the different tautomeric forms generally occur through mediated proton transfer reactions; simultaneous double proton transfer (e.g. between guanine and cytosine) have been proposed, albeit these conversions are generally energetically unfavorable. For example, the free energy difference between the canonical and imine forms obtained at the B3LYP/6-311G(d,p) level is only 7.6 kJ/mol, whereas the activation barrier for direct proton transfer from N8 to N3 is close to 165 kJ/mol. Hence, a protonated (cationic) intermediate will most definitely enhance the interconversion.

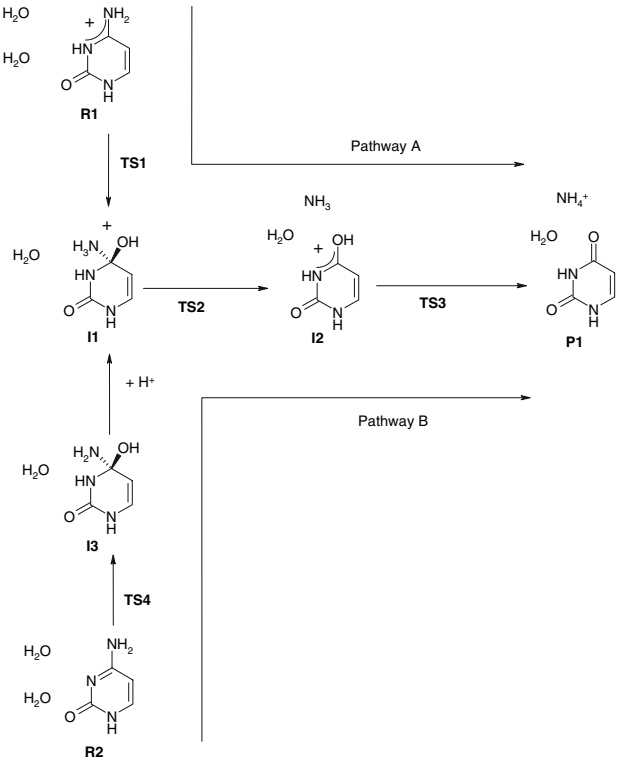

Fig. 2 Schematic outline of pathways A and B explored in the current work

3.1 Deamination resulting from N3 protonated form

The mechanism of the first deamination pathway (A) investigated is outlined schematically in Fig. 2. The reaction starts with the assumption that cytosine has become protonated at the N3 position (e.g., as an intermediate during the conversion between the amine–oxo and the imine tautomers). The computed proton affinity at the N3 position is at the current level of theory −1187.4 kJ/mol in aqueous PCM solvent, with a corresponding free energy of protonation in aqueous solution of −1150.0 kJ/mol. If we subtract the estimated free energy of a solvated proton, −1124.2 kJ/mol [51], we can conclude that even in aqueous solution, the normal cytosine appears to have a slightly exothermic proton affinity (ca −26 kJ/mol), and that it is not unlikely that the species can become protonated spontaneously. Once formed, addition of a water molecule across C4/N8 (step 1) produces an intermediate, I1, that readily looses ammonia through transition state 2. Ammonia in turn will abstract the remaining proton from the OH group (TS3) to produce uracil, water and an ammonium cation.

The initial step involves the formation of a strongly hydrogen bonded complex (R1) with two water molecules. The optimized structure is displayed in Fig. 3. In Table 1 we list the relative zero-point energies of reaction in vacuo, and the corresponding free energies in vacuo and in solvent. In R1, the hydrogen bond distance between the N3 proton and oxygen of the first water molecule is 1.82 Å, and the hydrogen bond between the two waters 1.98 Å. The oxygen of the first water lies 3.63 Å from C4 to which it will eventually bind. In the transition structure (TS1), water binds to C4 and simultaneously transfers one proton to the second water. This, in turn, functions as a proton shuttle, transferring one of its other protons to the N8 amine group. The motion associated with the imaginary frequency of the reaction coordinate is very distinct, and lies at $405i$ cm^{-1}. The TS is late in the C4–O binding and early in the N8–H binding, whereas the main part of the vibrational motion corresponding to the reaction coordinate lies in the shuttle of a proton between the two water oxygens Fig. 4.

Figure 5 shows the IRC energy profile corresponding to this step. It can be seen that it corresponds to a concerted mechanism involving six atoms, N8, C4, and two oxygen atoms and two hydrogen atoms of the water molecules. In the first intermediate formed, the remaining water molecule hydrogen bonds strongly to the NH_3 group (O–H distance 1.77 Å), and weakly to the N3 proton (O–H distance 2.22 Å).

Once formed, ammonia (N8) can leave by a simple TS, TS2, in which the C–N bond is elongated to 1.92 Å, with an imaginary frequency of $262i$ cm^{-1} for the reaction coordinate. The hydrogen bonds to the water molecule are retained, although elongated by 0.3–0.5 Å. The dissociated ammonia molecule remains hydrogen bonded to the added hydroxyl group, and resides on the opposite side of the ring compared

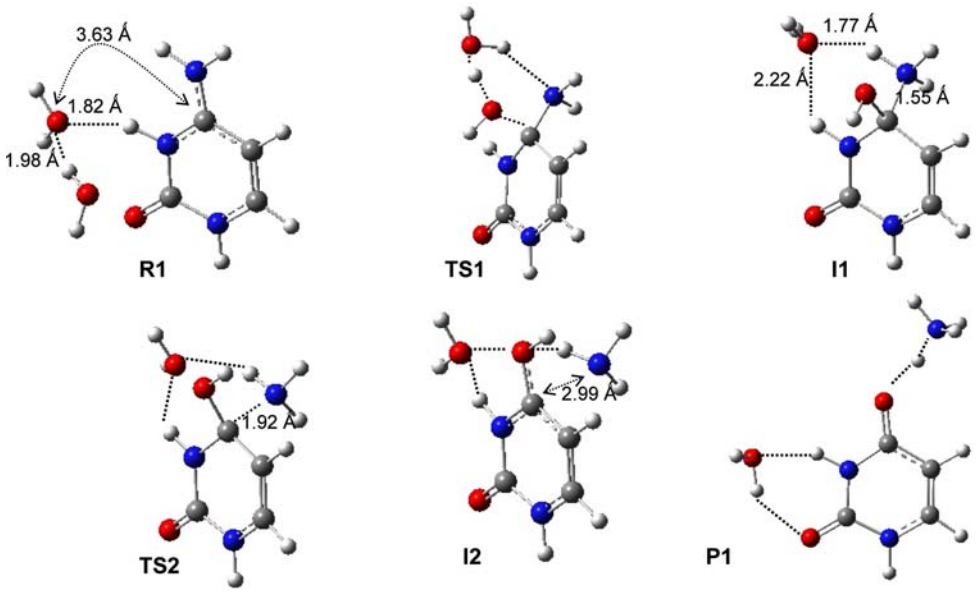

Fig. 3 PCM optimized stationary structures along pathway A

Table 1 Relative energies for deamination pathway A

System	ΔE_{vacuo}	$\Delta G^{298}_{\text{vacuo}}$	$\Delta G^{298}_{\text{aq}}$
R1	0.0	0.0	0.0
TS1	201.3	213.9	140.3
I1	130.1	137.9	74.5
TS2	136.7	143.9	91.8
I2	82.7	70.0	41.2
P1	5.4	2.2	−42.5

(ΔE_{vacuo} : relative zero-point energy in vacuo; $\Delta G^{298}_{\text{vacuo}}$: relative free energy in vacuo at 298 K; $\Delta G^{298}_{\text{aq}}$: relative free energy taking into account the PCM corrections at 298 K. All data in kJ/mol)

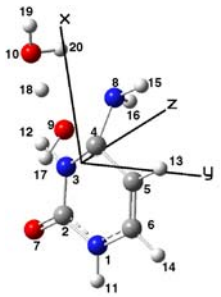

frequency : 405.1561**i* cm^{-1}

Atom label	Atom symbol	Normal coordinates X	Y	Z
1	N	0.00	0.00	0.00
2	C	0.00	0.00	0.00
3	N	0.01	0.01	0.00
4	***C***	***-0.06***	***0.00***	***0.12***
5	C	0.00	-0.01	-0.02
6	C	0.00	-0.01	-0.01
7	O	0.01	0.00	0.00
8	N	-0.05	0.03	0.03
9	***O***	***0.10***	***0.00***	***-0.03***
10	O	-0.02	-0.01	-0.06
11	H	0.00	0.00	-0.01
12	H	0.01	0.03	0.11
13	H	0.01	-0.01	0.01
14	H	0.00	0.00	-0.01
15	H	-0.02	0.02	0.02
16	H	-0.01	0.01	0.05
17	***H***	***0.21***	***-0.37***	***-0.05***
18	***H***	***-0.65***	***0.45***	***-0.05***
19	H	-0.04	-0.08	-0.12
20	***H***	***0.27***	***-0.16***	***-0.01***

Fig. 4 Vibrational mode corresponding to the imaginary frequency of TS1 in water

to the second water molecule. For the subsequent step, although a proton transfer from the C4 hydroxyl group to ammonia giving the final uracil–H_2O–NH_4^+ complex seems possible and thermodynamically favorable (P1 is more stable than I2 by 67.8 kJ/mol in vacuo and by 83.7 kJ/mol in water solvent), no transition state was found linking correctly the two minima.

Energetically, the free energy of activation of adding a water molecule across C4/N8 (TS1) in solvent is 140.3 kJ/mol starting from the initially formed complex (R1); see Table 1. The addition reaction is endergonic by 74.5 kJ/mol, and is followed by a barrier of 17.3 kJ/mol for the loss of ammonia (TS2). The intermediate complex thus formed lies 41.2 kJ/mol above the initial starting complex, whereas the deamination reaction step itself is exergonic by close to 33 kJ/mol. The final proton transfer to form uracil, water and an ammonium ion, is associated with a free energy of reaction of only −83.7 kJ/mol, and results in a complex that is 42.5 kJ/mol more stable than the initial complex.

Comparing the free energies in vacuo, the energetics differ slightly, albeit a similar energy contour is given. The first barrier is much more lower in solvent ($\Delta G^{\neq}_{\text{aq}} = 140.3$ kJ/mol) than the one in vacuo ($\Delta G^{\neq}_{\text{vacuo}} = 213.9$ kJ/mol), corresponding to a big stabilization of TS1 in water solvent. On the contrary, the deamination itself is easier in vacuo ($\Delta G^{\neq}_{\text{vacuo}} = 6.0$ kJ/mol) than in solvent ($\Delta G^{\neq}_{\text{aq}} = 17.3$ kJ/mol) because I1 is more stabilized in water than TS2.

The rate determining step is the initial addition reaction, and the value in solvent is somewhat higher than the experimentally reported activation energy of $E_a = 117 \pm 4$ kJ/mol [37]. This value remains, however, 15 kJ/mol lower than the lowest free energy barrier reported by Almatarneh et al. [40] for hydroxyl ion induced deamination at the G3MP2 level of theory. Comparing with the free energies obtained at the B3LYP/6-31G(d) level in their study, the rate determining

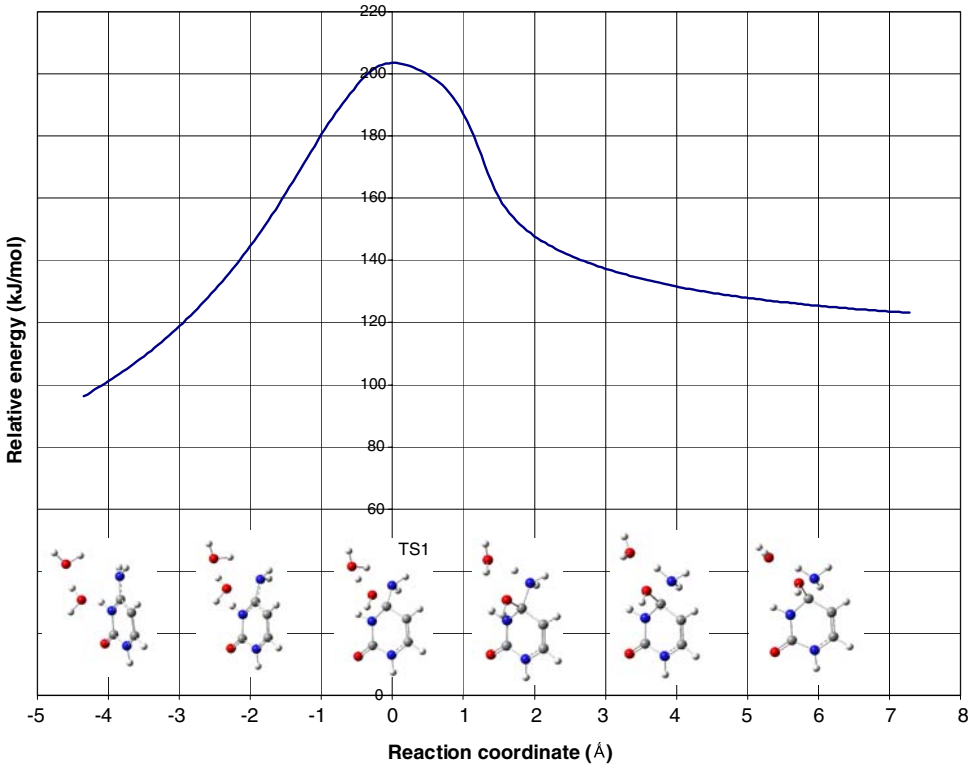

Fig. 5 IRC energy profile corresponding to the step R1→TS1→I1 in vacuo

step of the current pathway is 40 kJ/mol lower in energy, and hence poses an energetically much more viable pathway.

3.2 Water addition to neutral cytosine

Rather than pathway A, starting with protonated form of cytosine to which water is added, one can also imagine a mechanism in which a water molecule first adds to neutral cytosine (R2 → TS4 → I3), followed by protonation of the amino nitrogen (to give I1), after which the same route as pathway A will be followed from I1 onwards. Spontaneous deamination from neutral cytosine, in which the reaction sequence is initiated by the addition of a water molecule at C4 has also been explored by Almatarneh et al. [40] Two different reaction mechanisms were investigated in that study, in both cases considering neutral water catalyzed deamination (i.e. no hydroxyl anion involved). At all levels of theory, neither of these had a rate determining step less than 210 kJ/mol, and were thus concluded as being less likely. Instead, the most probable pathway explored therein involved initial attack by OH^- at C4, with a gas phase activation free energy ($\Delta G^{\neq}$) of 155.7 kJ/mol (G3MP2 level) and gas phase activation energy (ΔE_{act}) of 148.0 kJ/mol. The corresponding values at the B3LYP/6-31G(d,p) level were 180.3 kJ/mol and 177.3 kJ/mol, respectively. No environmental effects were, however, considered in that study.

In the current study, the initial complex R2 resembles R1 of pathway A, except that one of the water molecules is now a hydrogen bond donor to the N3 nitrogen (which is protonated in pathway A). Addition of the first water molecule to C4 occurs by simultaneous proton transfer to the second water, that in turn acts as a shuttle and protonates N3. The O_{water1}–C distance of TS4 is 2.24 Å, and the O_{water1}–H–O_{water2} distances 1.37 and 1.11 Å, respectively. The imaginary frequency is very similar to that of water addition in pathway A, 408*i* cm^{-1}. The barrier height (free energy) is at the current level of theory 156.3 kJ/mol in solvent and 162.1 kJ/mol in vacuo (see Table 2), i.e., much more lower than for the pathway in which protonation of N3 is undertaken before addition of water in vacuo, but slightly higher if the bulk solvent effect is taken into account. The reaction is endergonic by

Table 2 Relative energies for deamination pathway B

System	ΔE_{vacuo}	ΔG^{298}_{vacuo}	ΔG^{298}_{aq}
R2 + H^+	0.0	0.0	0.0
TS4 + H^+	153.1	162.1	156.3
I3 + H^+	90.7	94.1	98.5
I1	−876.5	−846.4	60.9
TS2	−869.9	−840.4	78.2
I2	−923.9	−914.3	27.5
P1	−1001.2	−982.1	−56.1

(ΔE_{vacuo} : relative zero-point energy in vacuo; ΔG^{298}_{vacuo}: relative free energy in vacuo at 298 K; ΔG^{298}_{aq}: relative free energy taking into account the PCM corrections at 298 K. All data in kJ/mol)

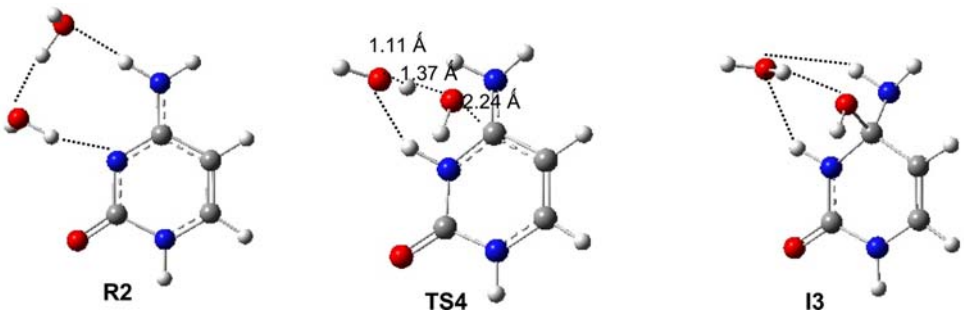

Fig. 6 PCM optimized structures of the initial steps of pathway B

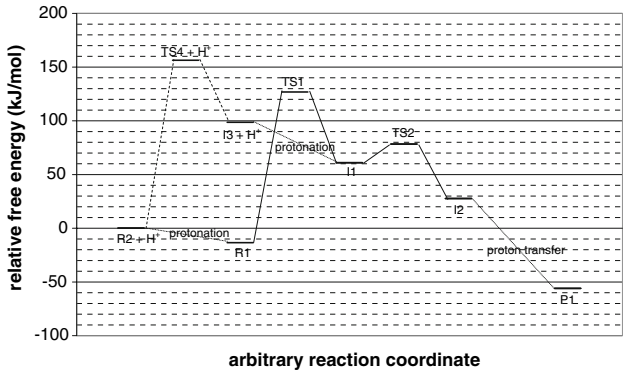

Fig. 7 Energetics of pathways A and B in the proton assisted hydrolytic deamination of cytosine. *Solid line* shows the evolution of the PCM corrected free energy in pathway A, and *dashed line* the PCMcorrected free energy specific to pathway B, at 298 K

98.5 kJ/mol in solvent and 94.1 kJ/mol in vacuo. The PCM optimized structures are depicted in Fig. 6.

The next step, according to this pathway, is to protonate the amino group, resulting in the same intermediate (I1) as after the first step of pathway A; all the subsequent steps will be the same as pathway A. The free energy of N8 protonation of the neutral water-added complex I3 in aqueous solution is exergonic by −1156 kJ/mol, which after subtraction of the energy of the solvated proton (−1,124.5 kJ/mol [51]) results in an overall exergonic protonation of −37.6 kJ/mol.

Figure 7 presents a comparison of the energetics of pathways A and B in solvent.

4 Conclusions

In this work, we have studied the reaction of the deamination of cytosine (to uracil) assuming a proton catalyzed hydrolytic mechanism, in the presence of an additional catalyzing water molecule. Two pathways are described, one resulting from the N3 protonated form and a second resulting from a water addition to the neutral cytosine. Both are four-step mechanisms and involve the same type of reactions but in a different order. The difference lies in the two initial steps leading to the same intermediate species (I1), with the subsequent processes being the same.

In the first pathway (A), there is first protonation at N3 of cytosine followed by a concerted water molecule addition at C4 with simultaneous proton transfer to the amino group leading to the intermediate species I1. The second route (B) involves an initial concerted addition of a water molecule to C4 and a simultaneous proton transfer to N3 followed by protonation of the amino group at N8, leading to the same intermediate as in pathway A. The two final steps, which are common to both pathways, include first elimination of the N8 ammonia group leading to a protonated uracil, followed by proton transfer from this last species to the ammonia giving an ammonium cation and neutral uracil.

In both pathways, the addition of water at C4 assisted by a second water molecule is the rate determining step. The addition to the protonated cytosine appears to be energetically favored over the addition to neutral cytosine, with calculated free energy barriers in aqueous solution of 140.3 and 156.3 kJ/mol, repsectively. This point indicates that the accelerated rate of deamination in acidic medium is related to the increased concentration of protonated cytosine. The activation free energy is slightly higher than the experimental value, yet closer than the theoretical values previously reported in the literature. This supports the concept that an additional catalytic water molecule plays an important role in the hydrolitic deamination of cytosine.

Acknowledgments The faculty of science and technology at Örebro University and the Swedish science research council (VR) is gratefully acknowledged for financial support (LAE).

References

1. Burgur A (1983) A Guide to the Chemical Basis of Drug Design. Wiley, New York
2. Peng W, Shaw BR (1996) Biochemistry 35:10172–10181
3. Florián J, Baumruk V, Leszczyński J (1996) J Phys Chem 100: 5578–5589
4. Sponer J, Leszczynski J, Hobza P (1996) J Comput Chem 117: 841–850
5. Estrin DA, Paglieri L, Corongiu G (1994) J Phys Chem 98:5653–5660

6. Scanlan MJ, Hillier IH (1984) J Am Chem Soc 106:3737–3745
7. Chandra AK, Nguyen MT, Zeegers-Huyskens T (2000) J Mol Struct (Theochem) 519:1–11
8. Chandra AK, Michalska D, Wysokinsky R, Zeegers-Huyskens T (2004) J Phys Chem A 108:9593–9600
9. Civcir PÜ (2000) J Mol Struc (Theochem) 532:157–169
10. Gould IR, Green DVS, Young P, Hillier IH (1992) J Org Chem 57:4434–4437
11. Morpurgo S, Bossa M, Morpurgo GO (2000) Adv Quantum Chem 36:169–183
12. Sambrano JR, Souza AR, Queralt JJ, Andrés J (2000) Chem Phys Lett 317:437–443
13. Colominas C, Luque FJ, Orozco M (1996) J Am Chem Soc 118: 6811–6821
14. Fogarasi G (2002) J Phys Chem A 106:1381–1390
15. Fogarasi G, Szalay PG (2002) Chem Phys Lett 356:383–390
16. Person WB, Szczepaniak K, Szczesniak M, Kwiatkowski JS, Hernandez L, Czerminski R (1989) J Mol Struc (Theochem) 194:239–258
17. Brown RD, Godfrey PD, McNaughton D, Pierlot AP (1989) J Am Chem Soc 111:2308–2310
18. Monajjemi M, Ghiasi R, Ketabi S, Passdar H, Mollaamin F (2004) pp 11–18
19. Monajjemi M, Ghiasi R, Abedi A (2005) Theor Inorg Chem 50:435–441
20. Burda J, Sponer J, Leszczynski J, Hobza P (1997) J Phys Chem B 101:9670–9677
21. Sponer J, Burda JV, Sabat M, Leszczynski J, Hobza P (1998) J Phys Chem A 102:5951–5957
22. Sponer JE, Miguel PJ, Rodruigez-Santiago L, Erxleben A, Krumm M, Sodupe M, Sponer J, Lippert B (2004) Angew Chem Int Ed 43:5396–5399
23. Russo N, Toscano M, Grand A (2001) J Phys Chem B 105:4735–4741
24. Russo N, Sicilia E, Toscano M, Grand A (2002) Int J Quantum Chem 90:903–909
25. Russo N, Toscano M, Grand A (2001) J Am Chem Soc 123:10272–10279
26. Russo N, Toscano M, Grand A (2003) J Mass Spectrom 38:265–270
27. Russo N, Toscano M, Grand A (2003) J Phys Chem A 107:11533–11538
28. Marino T, Toscano M, Russo N, Grand A (2004) Int J Quantum Chem 98:347–354
29. Marino T, Mazzuca D, Toscano M, Russo N, Grand A (2007) Int J Quantum Chem 107:311–317
30. Brown D, Phillips JH (1965) J Mol Biol 11:663–671
31. Notari RE, Chin ML, Cardoni A (1970) J Pharm Sci 59:27–32
32. Dreyfus M, Bensaude O, Dodin G, Dubois JE (1976) J Am Chem Soc 98:6338–6349
33. Shapiro R, Klein R (1966) Biochemistry 5:2358–2362
34. Chen H, Shaw BR (1994) Biochemistry 33:4121–4129
35. Glaser R, Rayat S, Lewis M, Son M-S, Meyer S (1999) J Am Chem Soc 121:6108–6119
36. Shapiro R, Klein R (1967) Biochemistry, 6:3576–3782
37. Frederico LA:, Kunkel TA, Shaw BR (1990) Biochemistry 29: 2532–2537
38. Lindahl T, Nyberg B (1974) Biochemistry 13:3405–3410
39. Duncan BK, Miller JH (1980) Nature 287:560–561
40. Almatarneh MH, Flinn CG, Poirier RA, Sokalski WA (2006) J Phys Chem A 110:8227–8234
41. Yao L, Li Y, Wu Y, Liu A, Yan H (2005) Biochemistry 44:5940–5947
42. Becke AD (1993) J Chem Phys 98:5648–5652
43. Lee C, Yang W, Parr RG (1988) Phys Rev B 37:785–789
44. McLean AD, Chandler GS (1980) J Chem Phys 72:5639
45. Krishnan R, Binkley JS, Seeger R, Pople JA (1980) J Chem Phys 72:650
46. Frisch MJ, Pople JA, Binkley JS (1984) J Chem Phys 80:3265
47. Cancès MT, Mennucci B, Tomasi J (1997) J Chem Phys 107: 3032–3041
48. Mennucci B, Tomasi J (1997) J Chem Phys 106:5151–5158
49. Cossi M, Scalmani G, Rega N, Barone V (2002) J Chem Phys 117:43–54
50. Frisch MJ, Trucks GW, Schlegel HB, Scuseria GE, Robb MA, Cheeseman JR, Montgomery JA Jr, Vreven T, Kudin KN, Burant JC, Millam JM, Iyengar SS, Tomasi J, Barone V, Mennucci B, Cossi M, Scalmani G, Rega N, Petersson GA, Nakatsuji H, Hada M, Ehara M, Toyota K, Fukuda R, Hasegawa J, Ishida M, Nakajima T, Honda Y, Kitao O, Nakai H, Klene M, Li X, Knox JE, Hratchian HP, Cross JB, Adamo C, Jaramillo J, Gomperts R, Stratmann RE, Yazyev O, Austin AJ, Cammi R, Pomelli C, Ochterski JW, Ayala PY, Morokuma K, Voth GA, Salvador P, Dannenberg JJ, Zakrzewski VG, Dapprich S, Daniels AD, Strain MC, Farkas O, Malick DK, Rabuck AD, Raghavachari K, Foresman JB, Ortiz JV, Cui Q, Baboul AG, Clifford S, Cioslowski J, Stefanov BB, Liu G, Liashenko A, Piskortz P, Komaromi I, Martin RL, Fox DJ, Keith T, Al-Laham MA, Peng CY, Nanayakkara A, Challacombe M, Gill PMW, Johnson B, Chem W, Wong MW, Gonzalez C, Pople JA. Gaussian 03, Revision C.02, Gaussian: Wallingford, 2004
51. Llano J, Eriksson LA (2002) J Chem Phys 117:10193–10206